Special Nuclear Material Characterization Using Digital 3-D Position Sensitive CdZnTe Detectors and High Purity Germanium Spectrometers

Michael Streicher, Steven Brown, Yuefeng Zhu, David Goodman, and Zhong He, *Senior Member, IEEE*

***Abstract*— Special nuclear material (SNM) monitoring often requires high resolution gamma-ray spectroscopy for material characterization. Portable systems and rapid deployment are also highly valued for some applications. Deployable gamma-ray imaging spectrometers using pixelated CdZnTe semiconductor detectors have become commercially available within the past three years to meet these requirements. CdZnTe systems have demonstrated room-temperature energy resolutions below 0.5% FWHM at 662 keV using single pixel events and below 0.7% FWHM at 662 keV using all events. The systems are able to go from storage to measurement in less than two minutes. Special nuclear materials were measured at the Y-12 National Security Complex and at the Device Assembly Facility at the Nevada National Security Site. The use of a CdZnTe system to measure uranium enrichment was demonstrated and uranium spectral features were compared to a commercially available high purity germanium (HPGe) spectrometer. The use of passive gamma-ray spectroscopy techniques to estimate plutonium grade using CdZnTe detectors was demonstrated for the first time.**

***Index Terms*— CdZnTe detectors, gamma-ray imaging, gamma-ray spectroscopy, special nuclear materials monitoring.**

I. Introduction

THE detection and characterization of special nuclear materials has applications in national and homeland security, safeguards, treaty verification, and emergency response [1]. In these applications, classifying the isotopic enrichment of the sample is extremely important. Measurement campaigns were conducted at the Y-12 National Security Complex and at the Device Assembly Facility (DAF) at the Nevada National Security Site to measure the enrichment of various uranium samples, to measure plutonium grade, and to image SNM sources in multiple configurations.

Spectrometers using $2 \times 2 \times 1.5$ cm^3 CdZnTe semiconductor detectors are excellent candidates to be used for rapid SNM characterization, especially in scenarios where material cannot be removed easily from a location for mass spectroscopy or active interrogation analysis. These conditions may exist during International Atomic Energy Agency (IAEA) inspections or international treaty verification. CdZnTe has demonstrated energy resolution below 0.5% FWHM for single pixel events at 662 keV [2]. The energy resolution at 185.7 keV has been measured in this work to be 1.55% FWHM. The intrinsic photopeak efficiency for 59.5 keV gamma rays for a cathode side irradiation is 99% and 11.2% at 662 keV [2]. For 185.7 keV gamma-rays, the intrinsic photopeak efficiency is 93% for a single detector. The photopeak efficiency can be improved by building larger tiled systems with multiple rows of detectors to capture the full energy from Compton scattering events. The capabilities of these sensors are significantly better than the previous generation of portable CdZnTe spectrometers [3], [4]. Thermal neutron detection, with gamma-ray spectroscopy, in a single compact instrument like the prototype system described in this work can further aid in the identification of special nuclear materials.

Manuscript received April 15, 2016; revised June 9, 2016; accepted June 26, 2016. Date of publication July 20, 2016; date of current version October 11, 2016. The digital 3-D Orion CdZnTe detector technology was developed under support from the U.S. Department of Defense, Defense Threat Reduction Agency under award #HDTRA1-12-C-0034. Any opinions, findings and conclusions or recommendations expressed in this material are those of the authors and do not necessarily reflect the views of the Defense Threat Reduction Agency. The U.S. Department of Energy, Office of Defense Nuclear Nonproliferation Research and Development provided access to the Y-12 and DAF facilities as well as travel support (Grant Award #DE-NA002131).

The authors are with the Department of Nuclear Engineering and Radiological Sciences, University of Michigan, Ann Arbor, MI 48109 USA (e-mail: streichm@umich.edu).

Color versions of one or more of the figures in this paper are available online at http://ieeexplore.ieee.org.

Digital Object Identifier 10.1109/TNS.2016.2593631

II. Detection System

A prototype digital CdZnTe array system was used during measurement campaigns at the DAF and Y-12. The system consisted of four $2 \times 2 \times 1.5$ cm^3 CdZnTe detectors grown by Redlen Technologies (Saanichton, British Columbia, Canada), each read out by a VAD_UM1.2 [5] application specific integrated circuit (ASIC) which was jointly developed by the University of Michigan and Integrated Detector Electronics AS (IDEAS) (Oslo, Norway). Each ASIC had 128 charge sensitive preamplifiers which read out 121 anode pixels on each detector as well as the signals induced on the planar cathode and the guard ring. The ASIC preamplifier output pulse waveforms were sampled at 40 MHz and digitally filtered using system reponse function fitting [6] in order to determine the signal amplitudes. Digitizing the pulse waveform is a departure from the analog signal processing methods used previously [7]. Interaction depths were calculated using the cathode-to-anode signal ratio (CAR) for single pixel events and using measured charge drift times for multiple pixel events [8]. The energy deposition of each interaction was calculated using the anode signal amplitude, depth corrected for electron trapping and weighting potential variation. The system consistently demonstrated energy resolutions below 0.5% FWHM at 662 keV for single pixel events and below 0.7% FWHM for all events [9]. Fig. 1 demonstrates the energy resolution of the system at 662 keV using all events.

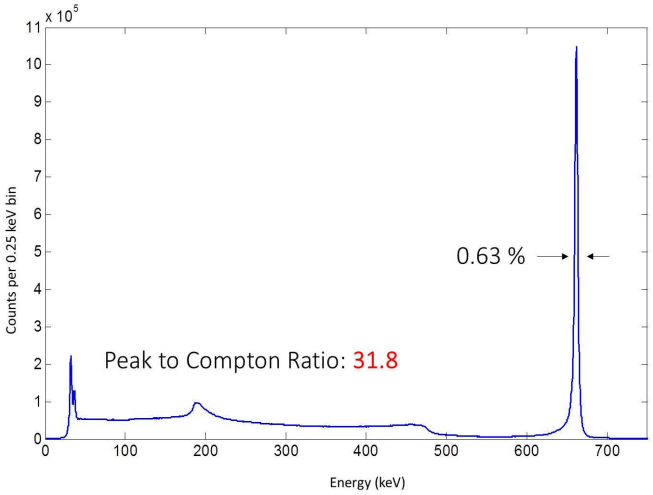

Fig. 1. ^{137}Cs gamma-ray spectrum recorded using the prototype digital CdZnTe array system. All events from four CdZnTe detectors are included in this spectrum. Note that the K_α and K_β x-rays from the cesium source can be resolved at 35 keV. The data were recorded at 2500 counts per second. A 30 μCi source was placed 10 cm from the detectors and data were recorded for 12 hours.

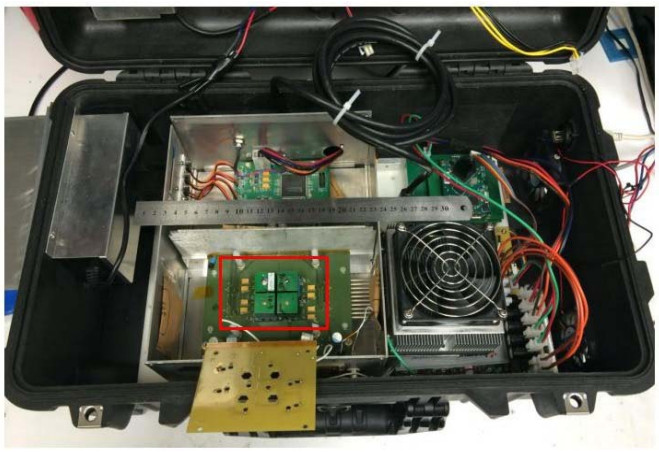

Fig. 2. Prototype digital array system. The location of the sensors within the housing case is shown with the red rectangle.

The system was self-contained in a 54 × 30 × 23 cm^3 Pelican ® case. The system communicated to a PC via USB connection and adapted 120 V AC power to DC in order to power the electronics. A Peltier cooler kept the system at 22 ^{o}C. A photograph of the system is shown in Fig. 2.

An ORTEC (Oak Ridge, TN) micro-detective hand-held radioisotope identifier [10] was used to simultaneously measure the samples to compare the energy resolution and efficiency of the commercial detector with the CdZnTe prototype. The p-type germanium detector was in a coaxial geometry, 50 mm in diameter and 33 mm in height.

III. Uranium Enrichment Measurement

Verifying uranium enrichment is critical in international safeguards for material accountancy. A knowledge of uranium enrichment can provide valuable insight into both the provenance and the likely end uses of recovered materials [11], [12]. However, due to weakly penetrating radiation and often

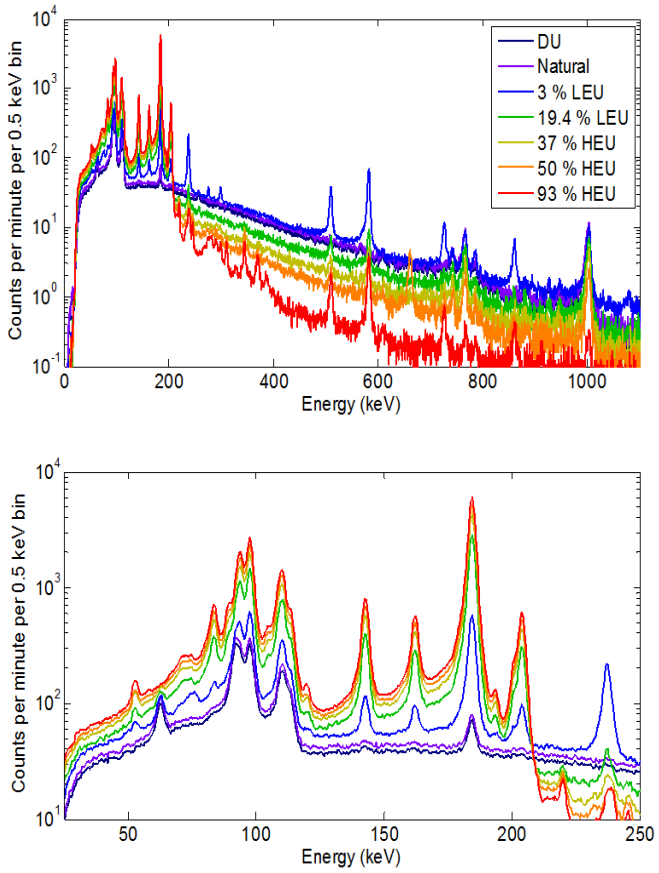

Fig. 3. Recorded all-events gamma-ray energy spectra from uranium metal disk samples of various enrichments. The sources were 3 cm in diameter and 3 mm thick. No background subtraction was carried out for the spectra presented.

unknown geometries, the enrichment is challenging to measure in realistic scenarios using gamma-ray spectroscopy [13].

Site 2 at the Y-12 Nuclear Detection and Sensor Testing Center provided eleven uranium metal samples with various enrichments. Each sample was a disk approximately 3 cm in diameter and 3 mm thick. The enrichment of the samples varied from 0.2 to 93.2 wt% ^{235}U [14]. Fig. 3 shows the measured spectra for samples of uranium with various enrichments measured using the prototype system. The 3 wt% ^{235}U sample had substantially more thorium than other samples which is characterized by a 2.6 MeV line as well as the prominent 238 keV line.

The strongest emission from ^{235}U is the 185.7 keV gamma ray with an intensity of 4.32 x 10^4 photons per second per gram of ^{235}U [11]. When the dimensions of the sample under investigation are known, dead-time corrected counting measurements of the 185.7 keV line are used to determine the enrichment of a sample [11], [15]–[18]. The calculated net photopeak area is affected by the photopeak efficiency of the detector as well as the energy resolution. A depleted uranium (DU) sample and a 93 wt% ^{235}U HEU sample were measured using the coaxial HPGe detector as well as the CdZnTe from the same distance in order to compare the efficiency and resolution of the detectors. Fig. 4 shows the spectra recorded using both detectors. The energy resolution of

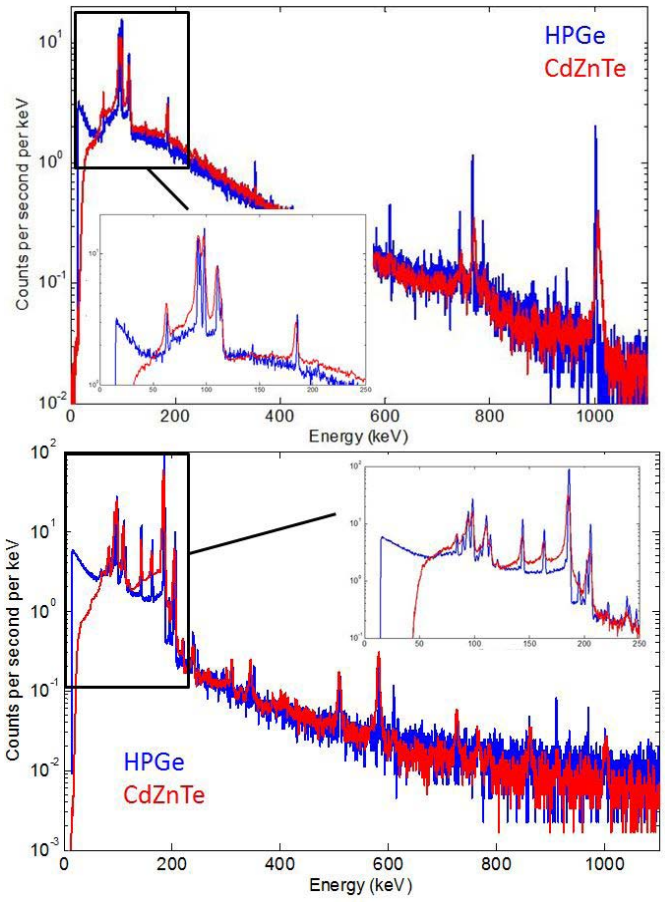

Fig. 4. Gamma-ray spectra from 0.2 wt% ^{235}U depleted uranium disk sample from 25 cm away recorded using prototype digital CdZnTe array system and a commercially available mechanically cooled HPGe detector (top) and spectra from 93 wt% ^{235}U HEU sample (bottom). The insets compare the recorded spectra between 0 and 250 keV. Many prominent ^{235}U gamma-ray lines are emitted in this energy range.

CdZnTe, while inferior to HPGe is sufficient to resolve almost all of the gamma-ray lines of interest. The net photopeak counts in each region of interest was used to compare the efficiency of HPGe and CdZnTe. Geant4 [19] was used to simulate the intrinsic photopeak efficiency of the two detectors. As shown in Fig. 5, the efficiency of CdZnTe is better at low gamma-ray energies. However, at higher energies, as multiple interaction Compton scattering becomes the dominant interaction mechanism, the larger HPGe detector has improved efficiency to capture the full energy from multiple scatters. The measured relative count rate roughly matches what is predicted from simulation as shown in Fig. 6. The energy resolution of the various uranium signatures are shown for both detectors in Fig. 7.

The relative errors in the net count rate of the 186 keV photopeak are 0.28% and 0.39% respectively for the HPGe detector and CdZnTe detector for the HEU sample. The uncertainty is greater for CdZnTe because the resolution is worse, so a larger background contribution must be subtracted. Likewise, the standard errors in the net count rate of the 186 keV photopeak from the DU sample are 1.3% and 3.6% for HPGe and CdZnTe.

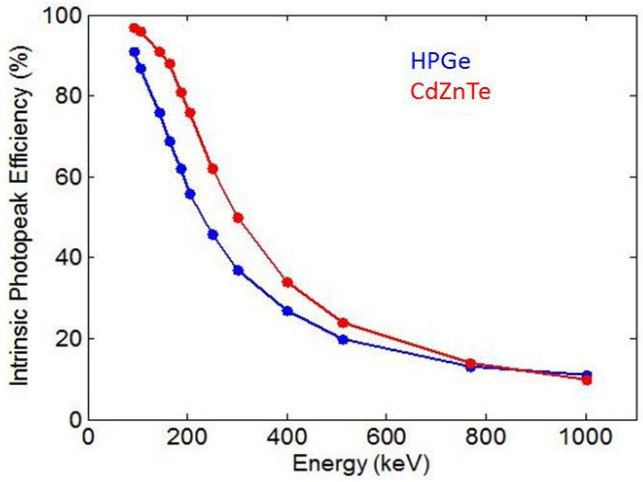

Fig. 5. Intrinsic photopeak efficiency for gamma-ray lines of interest for uranium measurements from Geant4 simulation.

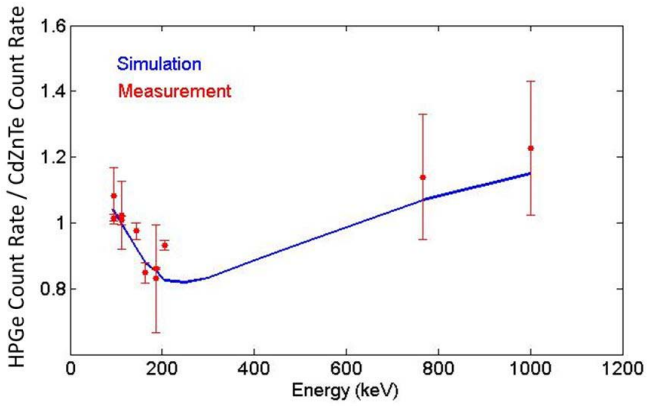

Fig. 6. Measured net count rate ratios for various uranium gamma-ray lines compared with the expected ratio from Geant4 simulation. The measured net photopeak count rates were calculated using the two spectra shown in Fig. 4 from depleted uranium and 93 wt% ^{235}U HEU samples.

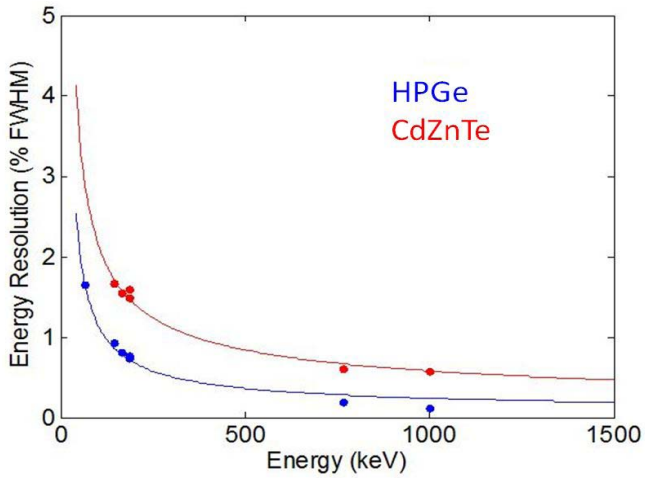

Fig. 7. Measured energy resolution of HPGe detector and CdZnTe array for characteristic uranium gamma-ray lines. The measured energy resolutions were calculated using the two spectra shown in Fig. 4 from depleted uranium and 93 wt% ^{235}U HEU samples.

In order to calculate the enrichment of the uranium samples, a method highlighted in the appendix was used to compare the photopeak count rates for the 1001 keV peak associated

TABLE I
ENERGIES AND BRANCHING RATIOS OF PHOTONS IN THE x-RAY REGION OF URANIUM SAMPLES

Photon Energy (keV)	Photon Source	Branching Ratio (%)
81.23	^{231}Th γ-ray (^{235}U)	0.89
82.09	^{231}Th γ-ray (^{235}U)	0.4
84.21	^{231}Th γ-ray (^{235}U)	6.6
89.95	^{231}Th γ-ray (^{235}U)	0.94
89.96	Th Kα_2 x-ray	-
92.28	Pa Kα_2 x-ray	-
92.38	^{234}Th γ-ray (^{238}U)	2.81
92.8	^{234}Th γ-ray (^{238}U)	2.77
93.35	Th Kα_1 x-ray	-
94.65	U Kα_2 x-ray	-
95.86	Pa Kα_1 x-ray	-
96.09	^{235}U γ-ray	0.086
98.43	U Kα_1 x-ray	-

with ^{238}U to the photopeak count rate of the 186 keV line that is a signature of ^{235}U. Using this method, the enrichment of the 0.2 wt% ^{235}U DU sample was estimated to be 0.19 $\pm$ 0.01 wt% ^{235}U using the spectrum recorded using the HPGe detector. The enrichment was estimated to be 0.19 $\pm$ 0.02 wt% ^{235}U using the spectrum recorded using the prototype digital CdZnTe array. The enrichment of the 93 wt% ^{235}U HEU sample was measured to be 91.3 $\pm$ 2.5 wt% ^{235}U using the HPGe detector. Using the CdZnTe array, the enrichment was estimated to be 87.8 $\pm$ 10.1 wt% ^{235}U. The resolution and efficiency of the HPGe detector is significantly better for the 1001 keV line. The superior detection of the 1001 keV line at high enrichments is a significant advantage for the HPGe detector.

Between 90 and 100 keV, signatures of both ^{238}U and ^{235}U are present [20]. The line energies and the source of the various lines are shown in Table I. The recorded spectrum in the x-ray region on the prototype system from various uranium samples is shown in Fig. 8. The energy resolution of CdZnTe detectors does allow one to measure the enrichment of a uranium sample by comparing the ratio of counts in the region between 95.5 keV and 106 keV (Region 2 in Fig. 8) and the region between 86 keV and 95.5 keV (Region 1 in Fig. 8) [21]. The enrichment can be determined from the ratio of counts in Region 2 to Region 1 because the impact of the ^{234}Th lines around 92 keV decrease as enrichment increases. The intensity of the Kα x-rays from uranium increases as enrichment increases, but the ratio of Kα_1 to Kα_2 does not change, so fewer events from ^{234}Th increases the ratio. At very high enrichments, the 89.95 keV γ-ray from ^{231}Th adds to the number of counts in Region 1, degrading the results. However, as demonstrated in Fig. 9, this method can effectively discriminate depleted uranium, natural uranium, low-enriched uranium (LEU), and highly-enriched uranium (HEU). The intrinsic photopeak efficiency of 1.5 cm thick CdZnTe detectors is more than 96% for photons at these energies, so no efficiency calibration is required for this method. Very thin samples may not produce enough x-rays to use this simple uranium enrichment measurement method.

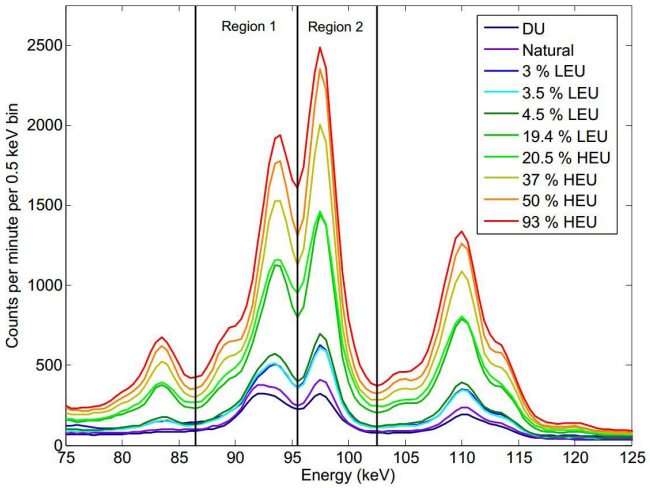

Fig. 8. Illustration of enrichment measurement using the uranium x-ray region. The two regions of interest in the spectrum are indicated for a number of different uranium samples.

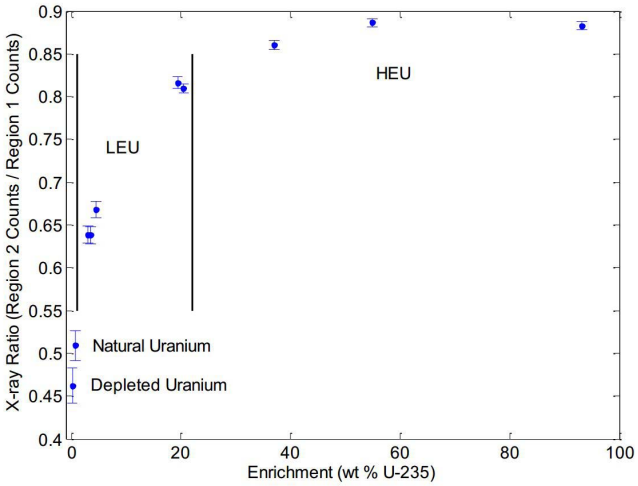

Fig. 9. Enrichment measurement using uranium x-ray emissions. Various regions of the x-ray ratio indicate different levels of uranium enrichment.

Contrastingly, the energy resolution of HPGe allows one to separate the characteristic gamma-ray lines in order to more accurately quantify the enrichment. As shown in Fig. 10, the germanium detector is able to resolve the gamma-ray lines around 92 keV which are characteristic of ^{238}U. Then, photopeak count ratios may be used to estimate the uranium enrichment by comparing the relative intensity of the gamma-ray lines characteristic of ^{238}U with the gamma-ray lines characteristic of ^{235}U (81.2 and 82 keV) [22].

IV. PLUTONIUM ISOTOPICS

Plutonium grade, much like uranium enrichment, determines whether the material can be used in a nuclear weapon. The plutonium grade can be measured using gamma-ray line photopeak ratios [11]. Most often, users are interested in the ratio between ^{239}Pu and ^{240}Pu because the spontaneous fission rate of ^{240}Pu limits the capability of the material to

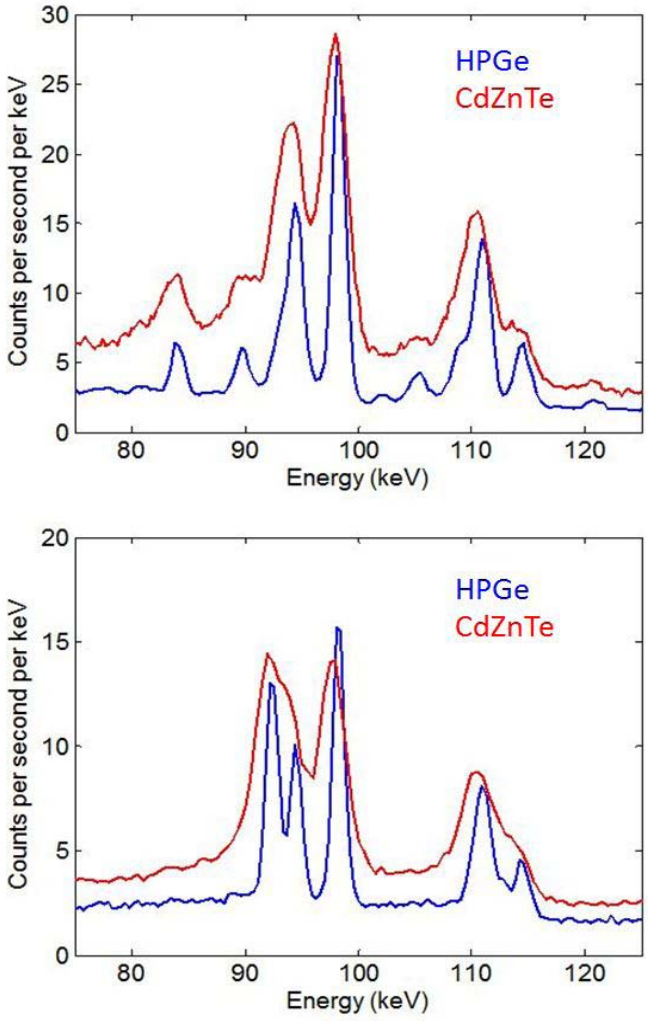

Fig. 10. Gamma-ray spectra from 93 wt% ^{235}U HEU disk sample from 25 cm away recorded using prototype digital CdZnTe array system and a commercially available mechanically cooled HPGe detector (top) and spectra from 0.2 wt % ^{235}U depleted uranium sample (bottom) focused on x-ray region (75-125 keV).

be weaponized. While many methods for measuring plutonium grade use ratios of lines below 200 keV [23], this work focuses on using the gamma-ray emissions between 630 and 670 keV to measure plutonium grade because these lines are significantly more penetrating. However, excellent energy resolution is required to discriminate the lines caused from the decay of three isotopes, ^{239}Pu, ^{240}Pu, and ^{241}Am [24]. Table II provides a list of gamma rays in this energy region.

Fig. 11 shows a comparison of the measured gamma-ray spectrum from a 5 kg disk of 95% ^{239}Pu recorded on the prototype system and the spectrum from the same object recorded with a field-deployable high-purity germanium gamma-ray spectrometer. Particularly between 300 and 450 keV, there are some distinct peaks in the HPGe spectrum that are unresolvable in the CdZnTe single pixel spectrum. Other notable differences include the more prominent 511 keV peak and 558 keV peak in the CdZnTe spectrum. The 558 keV peak arises from thermal neutron capture on ^{113}Cd. After thermal neutron capture on cadmium, a cascade of gamma

TABLE II

PHOTON SOURCES, ENERGIES, AND BRANCHING RATIOS FROM PLUTONIUM SAMPLES IN THE RANGE OF 630 keV TO 670 keV. SOURCE ISOTOPICS CAN BE ESTIMATED USING GAMMA-RAY LINES IN THIS ENERGY RANGE

Isotope	Energy (keV)	Branching Ratio (γ's per decay)	Activity (γ's / s-g)
^{241}Am	633.0	1.26 x 10^{-8}	1.59 x 10^{3}
^{239}Pu	633.2	2.53 x 10^{-8}	5.80 x 10^{1}
^{239}Pu	637.8	2.56 x 10^{-8}	5.87 x 10^{1}
^{239}Pu	640.1	8.20 x 10^{-8}	1.88 x 10^{2}
^{241}Am	641.4	7.10 x 10^{-8}	8.98 x 10^{3}
^{240}Pu	642.5	1.25 x 10^{-7}	1.05 x 10^{3}
^{239}Pu	646.0	1.49 x 10^{-7}	3.42 x 10^{2}
^{239}Pu	649.3	7.12 x 10^{-9}	1.63 x 10^{1}
^{239}Pu	650.5	2.70 x 10^{-9}	6.19 x 10^{0}
^{239}Pu	652.1	6.55 x 10^{-8}	1.50 x 10^{2}
^{241}Am	653.0	3.77 x 10^{-7}	4.77 x 10^{4}
^{239}Pu	654.9	2.25 x 10^{-8}	5.16 x 10^{1}
^{239}Pu	658.9	9.69 x 10^{-8}	2.22 x 10^{2}
^{241}Am	662.4	3.64 x 10^{-6}	4.61 x 10^{5}
^{239}Pu	664.6	1.66 x 10^{-8}	3.80 x 10^{1}
^{239}Pu	668.2	3.93 x 10^{-10}	9.02 x 10^{-1}

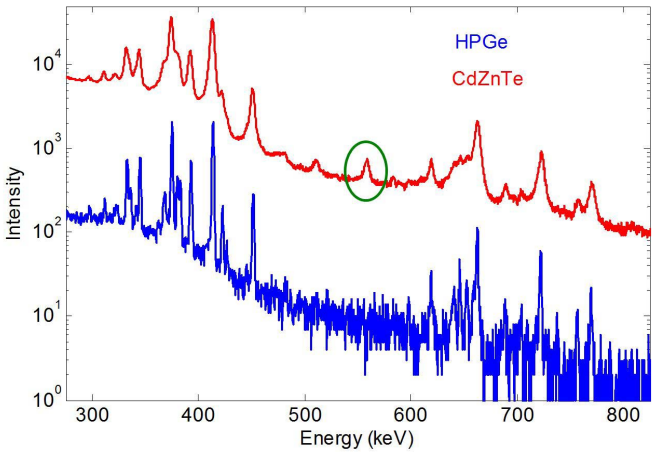

Fig. 11. Comparison of recorded gamma-ray spectrum from plutonium source recorded with a field-deployable HPGe detector and the prototype CdZnTe system. The 558 keV peak indicative of thermal neutron capture is shown circled in green.

rays are emitted, the most probable being at 558 keV which occurs in approximately 75% of all thermal neutron captures. The cross section for thermal neutron capture is large for ^{113}Cd such that 96% of thermal neutrons are absorbed within 1 mm of the surface of the CdZnTe detector. This is a useful indicator that a neutron source is present because even fast neutrons can thermalize in the environment and interact in the CdZnTe detector. HPGe does not have a comparable indicator of a neutron source. The 511 keV peak is also more prominent in the CdZnTe spectrum due to thermal neutron

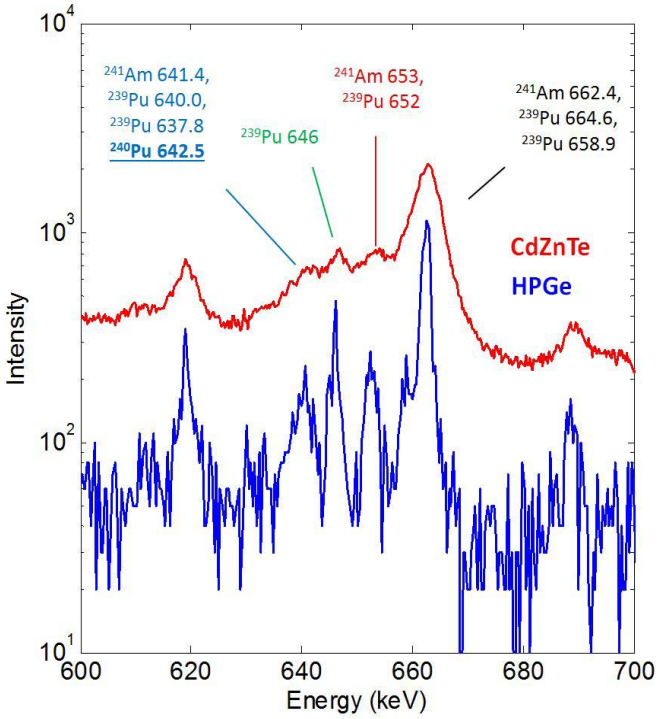

Fig. 12. Comparison of recorded gamma-ray spectrum from plutonium source recorded with a field-deployable HPGe detector and the prototype digital CdZnTe array system in the region where plutonium isotopics can be estimated. The four areas of interest are indicated.

capture on cadmium. The total energy released following a capture on cadmium is around 9 MeV meaning that some of the gamma rays emitted in the cascade will be of high energy (much greater than 1 MeV). These gamma rays are likely to undergo pair production in the environment which results in the higher number of annihilation photons. In addition, the plutonium source was driven with an AmBe neutron source during the CdZnTe measurement. This would have resulted in more fission gamma-rays which could have been the source of more annihilation photons in the CdZnTe spectrum.

In the 600 to 700 keV region, where the isotopics of plutonium can be ascertained, HPGe shows peaks with more separation as shown in Fig. 12. However, all of the peaks are similarly resolvable in both spectra. Some peaks that are not resolvable in CdZnTe are also unresolvable in HPGe. For instance, between 648 and 655 keV, there should be two separable lines; however, only one peak is present in both the CdZnTe and HPGe spectra. The separation is slightly better for the region between 655 and 665 keV using the HPGe sensor, but it is still very challenging to obtain different peak areas for each line.

In order to measure the fraction of ^{240}Pu in the sample, the relative intensity of ^{239}Pu must first be estimated from the 646 keV peak. This is a true signature of only ^{239}Pu content. Then, the relative amount of ^{241}Am can be estimated from the two peak regions between 650 keV and 665 keV. Finally, the ^{240}Pu content is estimated from the region between 635 keV and 642 keV accounting for the estimated quantities of ^{241}Am and ^{239}Pu calculated from the other regions. Los Alamos National Laboratory provided analysis assistance to estimate the plutonium grade using this general method and enhanced peak fitting. The result estimated the ratio of ^{240}Pu to total plutonium content to be 3.63% ± 1.02 %. The estimate was within 2σ of the true grade of 5.02%. Further improvement of energy resolution by using lower noise ASICs and improved CdZnTe material will improve the accuracy and precision of plutonium isotopic measurements.

The energy resolution of CdZnTe spectrometers has improved to the point where measuring plutonium isotopics is now possible. CdZnTe sensors also offer the advantage of indicating the presence of neutrons which is important for national and homeland security applications.

V. Conclusions

The excellent energy resolution demonstrated by CdZnTe sensors read out by digital ASICs can aid in the detection and characterization of SNM. The spectra from several special nuclear material samples recorded using a digital room-temperature 3-D position-sensitive CdZnTe imaging spectrometer were compared with the recorded spectra from HPGe detectors and demonstrate that CdZnTe can measure plutonium and uranium isotopics almost as well.

Appendix I
Peak Ratio Uranium Enrichment

The strongest emission from ^{238}U daughters is at 1001 keV with an intensity of 73.4 photons per second per gram of ^{238}U [11]. The ratio of the 186 keV line to the 1001 keV line provides an estimate of the sample enrichment, if one can estimate the extent of the source. The ratio of measured counts in the two lines is given in Equation (1).

$$\frac{\dot{m}_{186}}{\dot{m}_{1001}} = \left(\frac{E}{1-E}\right)\left(\frac{\dot{S}_{186}}{\dot{S}_{1001}}\right)\left(\frac{\epsilon_{pp186}}{\epsilon_{pp1001}}\right)\left(\frac{\varepsilon_{esc186}}{\varepsilon_{esc1001}}\right) \quad (1)$$

In Equation (1), $\dot{m}$ is the measured count rate of the indicated gamm-ray line and E is the enrichment of the sample. $\dot{S}$ is the source term for the gamma-ray line of interest (73.4 photons per second per gram for the 1001 keV line and 4.32 x 10^4 photons per second per gram for the 186 keV line). ϵ_{pp} is the absolute photopeak efficiency of the CdZnTe detector for the indicated gamma-ray line. ε_{esc} is the probability that a source photon of the indicated energy escapes from the source (avoids self-shielding). The detection efficiency ratio can be measured or simulated. For a four detector CdZnTe system, $(\epsilon_{pp186}/\epsilon_{pp1001}) = 9.4$ for source photons incident from the cathode side. For the HPGe detector, $(\epsilon_{pp186}/\epsilon_{pp1001}) = 5.9$. Contrastingly, escape probabilities requires a priori knowledge about the source or use of information about the source thickness from radiation images. The extent of the source, the source material (uranium metal, UO_2, etc.), and shielding around the source can change this ratio. For the samples measured at Y-12 with a thickness of 3 mm, $(\varepsilon_{esc186}/\varepsilon_{esc1001}) = 0.15$. This can be calculated in simple cases, by evaluating Equation (2).

$$\left(\frac{\varepsilon_{escape186\ keV}}{\varepsilon_{escape1001\ keV}}\right) \approx \frac{\int_0^D e^{-\mu_{186\ keV}x}dx}{\int_0^D e^{-\mu_{1001\ keV}x}dx} \quad (2)$$

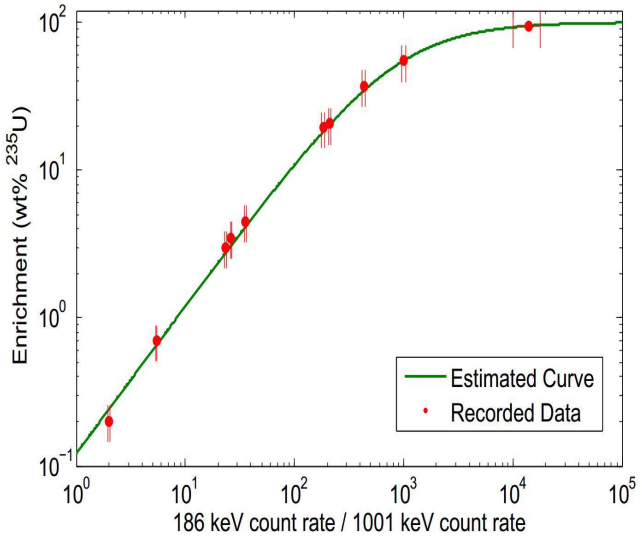

Fig. 13. Estimated enrichment curve for the source geometry used at the Y-12 National Security Complex. The measured results match the estimated values quite well. This demonstrates that the count rate ratio can be used to predict the enrichment of an unknown sample if the source geometry is known.

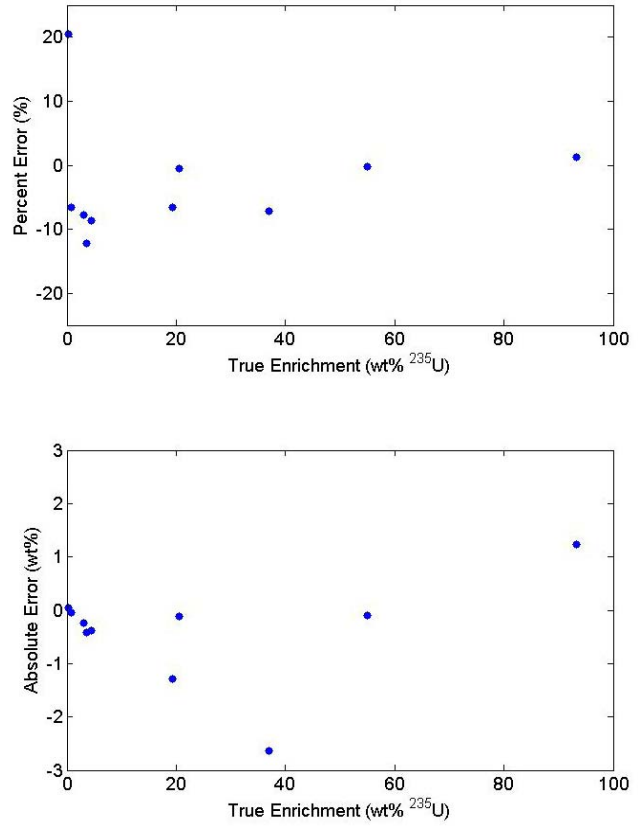

Fig. 14. Relative error between calculated enrichment using the peak ratio technique and the declared enrichment (top). The absolute error in wt% ^{235}U between the calculated enrichment and the declared enrichment (bottom).

In Equation (2), D is the thickness of the source material and μ is the total attenuation coefficient for the photon energy of interest. In realistic measurement scenarios, the thickness of the sample could be estimated using multiple views of the sample using coded aperture gamma-ray imaging. The attenuation coefficient could be estimated by measuring the relative attenuation of the higher energy lines from ^{238}U daughters using photopeak ratios. Equation (1) can be manipulated to calculate the enrichment of the source given the photopeak ratio. The data and the expected distribution of the enrichment as a function of the peak ratio is given in Fig. 13. Fig. 14 shows the relative error and the absolute error between the calculated enrichment using the described peak ratio technique and the declared enrichment of the sample. Using this method, the enrichment is correctly estimated to within 7% error on average. The largest discrepancy in this model is at 0.2 wt% ^{235}U where the measurement result is incorrect by 20% due to poor statistics for the 186 keV photopeak region.

ACKNOWLEDGMENT

The authors would like to thank the Y-12 National Security Complex for organizing the uranium measurement campaign, especially Dr. Carter Hull and Dr. Martin Williamson for organizing the campaign, and Dr. Joe Cochran, Barak Tjader, and Dr. Russell Hallman for escorting and material handling. The authors would also like to thank the entire Consortium for Verification Technology (CVT) for organizing the measurement campaign at the Device Assembly Facility. Special thanks to Prof. John Mattingly from North Carolina State University for organizing university groups to attend the measurements and to Prof. Sara Pozzi from the University of Michigan for leading the CVT Consortium. Thank you to Jesson Hutchinson and Derek Dinwiddie for organizing the effort from Los Alamos National Laboratory (LANL) staff to attend and facilitate the measurements. Scott Garner of Los Alamos National Laboratory provided valuable help regarding plutonium spectroscopy and provided analysis using a LANL spectral fitting program to estimate plutonium grade from the recorded gamma-ray spectrum. They would like to also thank Will Koehler of the University of Michigan for his editorial assistance.

REFERENCES

[1] "Nuclear security systems and measures for the detection of nuclear and other radioactive material out of regulatory control," Int. Atomic Energy Agency, Vienna, Austria, Tech. Rep. 21, 2013.

[2] F. Zhang, C. Herman, Z. He, G. De Geronimo, E. Vernon, and J. Fried, "Characterization of the H3D ASIC readout system and 6.0 cm^3 3-D position sensitive CdZnTe detectors," *IEEE Trans. Nucl. Sci.*, vol. 59, no. 1, pp. 236–242, Feb. 2012.

[3] D. T. Vo, "Comparison of portable detectors for uranium enrichment measurements," Los Alamos Nat. Lab., Los Alamos, NM, USA, Tech. Rep. LA-UR-06 2645, 2006.

[4] A. E. Proctor and K. R. Pohl, "Comparison of several detector technologies for measurement of special nuclear materials," Constellation Technol. Corp., Largo, FL, USA, Tech. Rep., 2003.

[5] Y. Zhu and Z. He, "Performance of a 2-keV digitizer ASIC for 3-D position-sensitive pixellated semiconductor detectors," in *Proc. Nucl. Sci. Symp. Med. Imag. Conf.*, Oct. 2012, pp. 4109–4112.

[6] Y. Zhu, "Digital signal processing methods for pixelated 3-D position sensitive room-temperature semiconductor detectors," Ph.D. dissertation, Univ. Michigan, Ann Arbor, MI, USA, 2012.

[7] F. Zhang, Z. He, G. F. Knoll, D. K. Wehe, and J. E. Berry, "3-D position sensitive CdZnTe spectrometer performance using third generation VAS/TAT readout electronics," *IEEE Trans. Nucl. Sci*, vol. 52, no. 5, pp. 2009–2016, Oct. 2005.

[8] Z. He *et al.*, "1-D position sensitive single carrier semiconductor detectors," *Nucl. Instrum. Methods, Phys. Res. A*, vol. 380, nos. 1–2, pp. 228–231, 1996.

[9] M. Streicher *et al.*, "A portable 2 × 2 digital 3D CZT imaging spectrometer system," in *Proc. Nucl. Sci. Symp. Med. Imag. Conf.*, Nov. 2014, pp. 1–3.
[10] Microdetective. [Online]. Available: http://www.ortec-online.com/download/Micro-Detective.pdf
[11] D. Reilly, N. Ensslin, H. Smith, Jr., and S. Kreiner, "Passive nondestructive assay of nuclear materials," Los Alamos Nat. Lab., Los Alamos, NM, USA, Tech. Rep. NUREG/CR-5550 LA-UR–90-732, 1991.
[12] C. T. Nguyen and J. Zsigrai, "Basic characterization of highly enriched uranium by gamma spectrometry," *Nucl. Instrum. Methods, Phys. Res. B*, vol. 246, no. 2, pp. 417–424, 2006.
[13] R. Berndt, E. Franke, and P. Mortreau, "^{235}U enrichment or UF6 mass determination on UF6 cylinders with non-destructive analysis methods," *Nucl. Instrum. Methods, Phys. Res. A*, vol. 612, no. 2, pp. 309–319, 2010.
[14] J. A. Cantrell, "Uranium enrichment standards of the Y-12 nuclear detection and sensor testing center," in *Proc. 52nd Annu. INMM Meeting*, 2012.
[15] K. Ianakiev *et al.*, "Advanced technology for enrichment monitoring in UF6 gas centrifuge enrichment plants," Los Alamos Nat. Lab., Los Alamos, NM, USA, Tech. Rep. LA-UR 10-06263, 2010.
[16] "Standard test method for measurement of ^{235}U fraction using enrichment meter principle," ASTM, Philadelphia, PA, USA, Tech. Rep. C1514-08, 2008.
[17] L. A. Kull and R. O. Ginaven, "Guidelines for gamma-ray spectroscopy measurements of ^{235}U enrichment," Brookhaven Nat. Lab., Upton, NY, USA, Tech. Rep. BNL 50414, 1974.
[18] T. Burr, S. Croft, and K. Jarman, "Uncertainty quantification in application of the enrichment meter principle for nondestructive assay of special nuclear material," *J. Sensors*, vol. 2015, Jun. 2015, Art. no. 267462.
[19] S. Agostinelli *et al.*, "Geant4—A simulation toolkit," *Nucl. Instrum. Methods, Phys. Res. A*, vol. 506, no. 3 pp. 250–303, 2003.
[20] H. Yücel and H. Dikmen, "Uranium enrichment measurements using the intensity ratios of self-fluorescence X-rays to 92* keV gamma ray in UXK$_\alpha$ spectral region," *Talanta*, vol. 78, no. 2, pp. 410–417, 2009.
[21] K. Abbas, J. Morel, M. Etcheverry, and G. Nicolaou, "Use of miniature CdZnTe X$_\gamma$ detector in nuclear safeguards: Characterisation of spent nuclear fuel and uranium enrichment determination," *Nucl. Instrum. Methods, Phys. Res. A*, vol. 405, no. 1, pp. 153–158, 1998.
[22] R. Gunnink *et al.*, "MGAU: A new analysis code for measurement ^{235}U enrichments in arbitrary samples," Lawrence Livermore Nat. Lab., Livermore, CA, USA, Tech. Rep. UCRL-JC-114713, 1994.
[23] T. E. Sampson, S.-T. Hsue, J. L. Parker, S. S. Johnson, and D. Bowersox, "The determination of plutonium isotopic composition by gamma-ray spectroscopy," *Nucl. Instrum. Methods*, vol. 193, nos. 1–2, pp. 177–183, 1982.
[24] T. Dragnev and K. Scharf, "Non-destructive gamma spectrometry measurement of 239Pu/240Pu and Pu/240Pu ratios," *Int. J. Appl. Radiat. Isot.*, vol. 26, no. 3, pp. 125–129, 1975.
[25] H. Yang, F. Zhang, Y. Zhu, and Z. He, "Efficiency measurement on 6.0 cm^3 3-D CdZnTe detectors," in *Proc. IEEE Nucl. Sci. Symp. Med. Imag. Conf.*, Oct./Nov. 2010, pp. 3756–3758.